

# **Determining How Much Topographic Complexity Must Be Incorporated into Models for Depositional Turbidity Currents Filling Sinuous Submarine Channels and Constructing Channel Levees\***

**Aymeric-Pierre Peyret<sup>1</sup>, David Mohrig<sup>1</sup>, Michael Lamb<sup>2</sup>, and Brandon McElroy<sup>1</sup>**

Search and Discovery Article #50368 (2010)

Posted December 17, 2010

\*Adapted from oral presentation at AAPG Annual Convention and Exhibition, New Orleans, Louisiana, April 11-14, 2010

<sup>1</sup>Jackson School of Geosciences, Univ. of Texas at Austin, Austin, TX ([aymeric.peyret@austin.utexas.edu](mailto:aymeric.peyret@austin.utexas.edu))

<sup>2</sup>Geological and Planetary Sciences, California Institute of Technology, Pasadena, CA.

## **Abstract**

Predicting spatial change in the thickness and grain size of turbidites away from points of well or outcrop control is a primary component of any quantitative model for deep-water stratigraphy. These predictions are often made using a numerical model that couples sediment transport and deposition to the flow field of a representative turbidity current. We present a methodology that can be used to evaluate how precisely this flow field must be described in order to accurately reconstruct thickness and grain size trends and apply the methodology to the modeling of turbidites filling sinuous submarine channels and constructing levees of submarine channels. To evaluate the control that local flow dynamics and channel topography have on depositional patterns, we calculate a characteristic advection length for every particle size of interest within a transporting turbidity current. This advection length is the horizontal length scale over which a representative particle is transported within the current between contacts with the bed. Its magnitude is the product of a characteristic travel time and a characteristic advection velocity. We estimate the advection time as a characteristic height above the bed associated with the suspended particles, divided by their representative settling velocity. The advection velocity is the average current velocity associated with the portion of the flow through which the grains are settling. We present laboratory and seismic data to demonstrate that deposit geometries are relatively insensitive to local channel topography and local flow dynamics for that part of the sediment load where the advection length scale is large relative to the imposed spatial changes. We then present a set of calculations defining the range of flows and particle sizes where depositional models for sinuous submarine channels and levees must include a description for deposition rate that is governed by gradients in local sediment transport capacity, versus flows and particle sizes where deposition rate can be prescribed to non-local sediment advection from upslope. Preliminary investigation indicates that gross depositional trends for turbidites composed of very fine and fine sand can almost always be modeled using a simple advection-settling model, while coarse sand typically requires inclusion of local dynamics; medium-sand turbidites are case specific.

## References

- Clark, J.D., and K.T. Pickering, 1996, Submarine Channels: Processes and Architecture: Vallis Press, London, 231 p.
- Clark, J.D., and K.T. Pickering, 1996, Architectural elements and growth patterns of submarine channels: Application to hydrocarbon exploration, AAPG Bulletin, v. 80/2, p. 194-221.
- Dietrich, W.E., 1982, Settling velocity of natural particles: Water Resources Research, v. 18/6, p. 1615-1626.
- Garcia, M.H., 1993, Hydraulic jumps in sediment-driven bottom currents: Journal of Hydraulic Engineering-ASCE, v.119/10, p. 1094-1117.
- Garcia, M.H., 1994, Depositional turbidity currents laden with poorly sorted sediment: Journal of Hydraulic Engineering-ASCE, v. 120/11, p. 1240-1263.
- Lamb, M.P., B. McElroy, B. Kopriva, J. Shaw, and D. Mohrig, 2010, Linking river-flood dynamics to hyperpycnal-plume deposits: Experiments, theory, and geological implications: GSA Bulletin, v. 122/9-10, p. 1389-1400.
- Pirmez, C., and J. Imran, 2003, Reconstruction of turbidity currents in Amazon channel: Marine and Petroleum Geology, v. 20/6-8, p. 823-849.
- Skene, K.I., D.J.W. Piper, and P.S. Hill, 2002, Quantitative analysis of variations in depositional sequence thickness from submarine channel levees: Sedimentology, v. 49/6, p. 1411-1430.
- Straub, K.M., and D. Mohrig, 2008, Quantifying the morphology and growth of levees in aggrading submarine channels: Journal of Geophysical Research-Earth Surface, v. 113, 20 p.

# Determining How Much Topographic Complexity Must Be Incorporated into Models for Depositional Turbidity Currents Filling Sinuous Submarine Channels and Constructing Channel Levees

Aymeric-Pierre Peyret, David Mohrig, Michael Lamb, Brandon McElroy

April 12, 2010

## 1 Why?

- Motivation
- Examples

## 2 How?

- Physical model
- Computational transcription

## 3 Results

- Advection length scales
- Influence of initial grain size distribution
- Computed lengths vs. literature

## 4 Conclusions

# Outline

## 1 Why?

- Motivation
- Examples

## 2 How?

- Physical model
- Computational transcription

## 3 Results

- Advection length scales
- Influence of initial grain size distribution
- Computed lengths vs. literature

## 4 Conclusions

## (1/2) Goals

- Simplification of models
- Applied to depositional turbidity currents
- Based on concept of particle advection length
- Allows one to model deposition very easily.

## (2/2) Modeling

- Current modeling tools model the whole flow field
  - Complex codes
  - Complicated flow field means computationally intensive programs, but
- A complicated flow field does not always transcribe to a very complicated deposition pattern
- What if, for certain cases, we could avoid computing the whole flow field?

# Outline

## 1 Why?

- Motivation
- Examples

## 2 How?

- Physical model
- Computational transcription

## 3 Results

- Advection length scales
- Influence of initial grain size distribution
- Computed lengths vs. literature

## 4 Conclusions

# (1/2) García's experiments

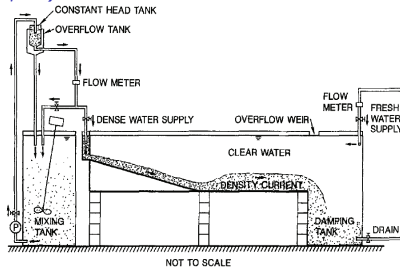
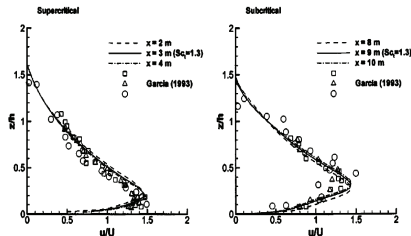


FIG. 2. Schematic of Experimental Facility

From García, 1993 & 1994 ([1], [2])

Diagram illustrating a laboratory experiment setup for studying density currents. The setup includes a constant head tank, an overflow tank, a flow meter, a mixing tank, a dense water supply, a clear water supply, a density current interface, a damping tank, and a drain. The diagram shows the flow of dense and clear water, the formation of a density current, and the measurement of flow rates.

**FIG. 2. Schematic of Experimental Facility**



From García, 1993 & 1994 ([1], [2])

# (1/2) García's experiments

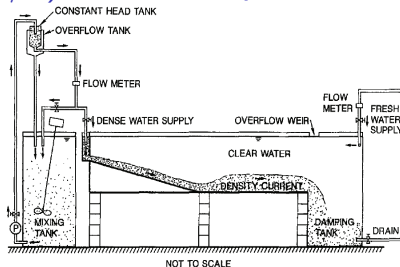


FIG. 2. Schematic of Experimental Facility

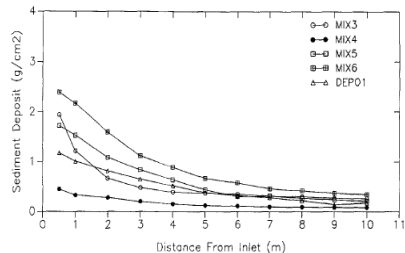
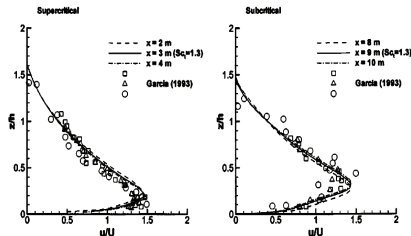


FIG. 7. Depositional Patterns Produced by Currents Driven by Poorly Sorted Sediment



From García, 1993 & 1994 ([1], [2])

# (1/2) García's experiments

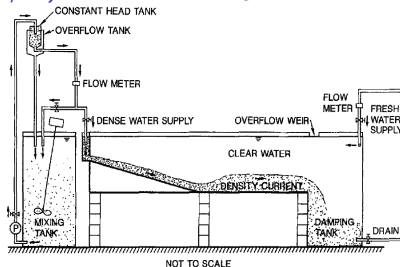


FIG. 2. Schematic of Experimental Facility

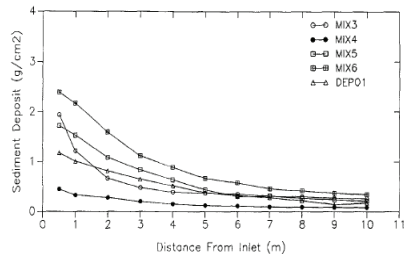
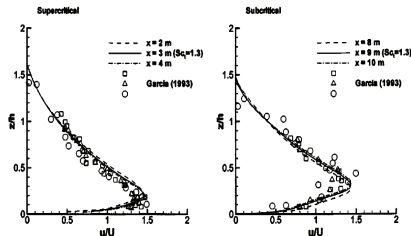


FIG. 7. Depositional Patterns Produced by Currents Driven by Poorly Sorted Sediment

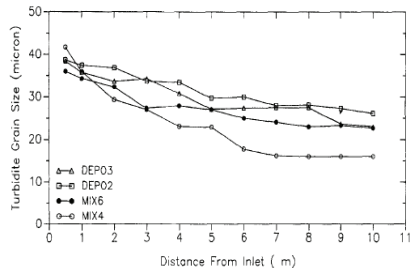
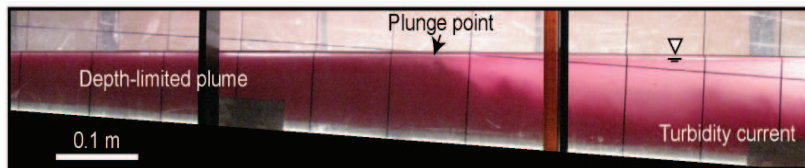


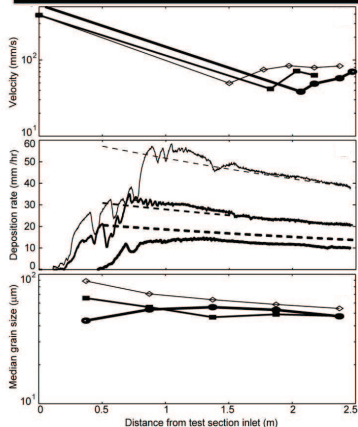
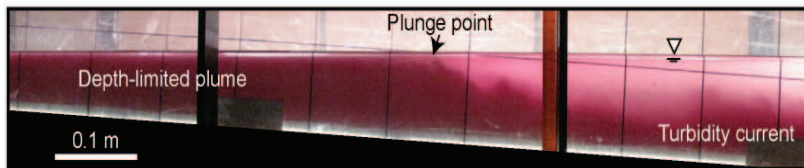
FIG. 8. Variation of Sediment Deposit Median Grain Size  $D_{50}$  with Distance from Inlet

From García, 1993 & 1994 ([1], [2])

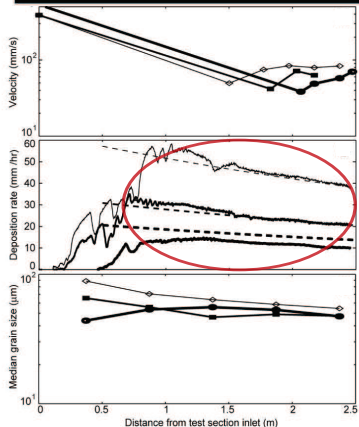
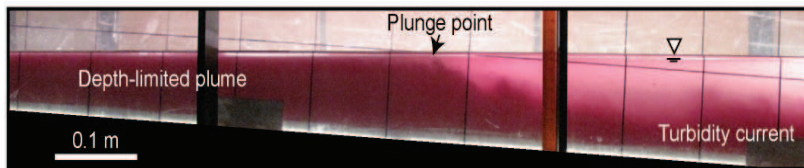
## (2/2) Lamb's experiments



## (2/2) Lamb's experiments



## (2/2) Lamb's experiments



From Lamb *et al.*, 2010 [3]

# Outline

## 1 Why?

- Motivation
- Examples

## 2 How?

- Physical model
- Computational transcription

## 3 Results

- Advection length scales
- Influence of initial grain size distribution
- Computed lengths vs. literature

## 4 Conclusions

# (1/3) Physical description

Let's start with:

$$(1 - \lambda_p) \cdot \frac{d\eta}{dt} = -\frac{dq_s}{dx} \text{ with } \begin{cases} \lambda_p & : \text{ bed porosity} \\ \eta & : \text{ bed elevation} \\ q_s & : \text{ volumetric sediment flux per unit width} \end{cases},$$

$$\frac{dq_s}{dx} = e \cdot w_s - c_b \cdot w_s \text{ with } \begin{cases} e & : \text{ dimensionless entrainment parameter} \\ c_b & : \text{ near-bed sediment concentration} \\ w_s & : \text{ particle settling velocity} \end{cases}$$

# (1/3) Physical description

Let's start with:

$$(1 - \lambda_p) \cdot \frac{d\eta}{dt} = -\frac{dq_s}{dx} \text{ with } \begin{cases} \lambda_p & : \text{ bed porosity} \\ \eta & : \text{ bed elevation} \\ q_s & : \text{ volumetric sediment flux per unit width} \end{cases},$$

$$\frac{dq_s}{dx} = e \cdot w_s - c_b \cdot w_s \text{ with } \begin{cases} e & : \text{ dimensionless entrainment parameter} \\ c_b & : \text{ near-bed sediment concentration} \\ w_s & : \text{ particle settling velocity} \end{cases}$$

and add two other equations

$$\begin{cases} q_s = c \cdot q \\ q_{sc} = c_c \cdot q \end{cases}, \text{ with } \begin{cases} c & : \text{ depth-averaged sediment concentration} \\ c_c & : \text{ depth-averaged sediment concentration at capacity} \\ q & : \text{ flow discharge per unit width} \\ q_{sc} & : \text{ sediment transport capacity per unit width} \end{cases}$$

## (2/3) Physical description

At capacity:

$$\left. \begin{aligned} \frac{dq_s}{dx} = w_s \cdot (e - c_b) = 0 \implies e = c_b \\ c = c_c \end{aligned} \right\} \implies c_c = \frac{e}{c_b} \cdot c = e \cdot \underbrace{\frac{c}{c_b}}_{\frac{1}{r_0}} \implies \underbrace{q \cdot c_c}_{q_{sc}} = q \cdot \frac{e}{r_0}$$

Combine all these equations:

$$\frac{dq_s}{dx} = w_s \cdot (e - c_b) = w_s \cdot \left( \frac{r_0 \cdot q_{sc}}{q} - \frac{c_b}{c} \cdot \frac{c \cdot q}{q} \right) = w_s \cdot \left( \frac{r_0 \cdot q_{sc}}{q} - \frac{r_0 \cdot q_s}{q} \right)$$

$$\left( \frac{q}{r_0 \cdot w_s} \right) \frac{dq_s}{dx} = q_{sc} - q_s \implies \text{Define: } l_a = \left( \frac{q}{r_0 \cdot w_s} \right) \implies \boxed{l_a \frac{dq_s}{dx} = q_{sc} - q_s}$$

## (2/3) Physical description

At capacity:

$$\left. \begin{aligned} \frac{dq_s}{dx} = w_s \cdot (e - c_b) = 0 \implies e = c_b \\ c = c_c \end{aligned} \right\} \implies c_c = \frac{e}{c_b} \cdot c = e \cdot \underbrace{\frac{c}{c_b}}_{\frac{1}{r_0}} \implies \underbrace{q \cdot c_c}_{q_{sc}} = q \cdot \frac{e}{r_0}$$

Combine all these equations:

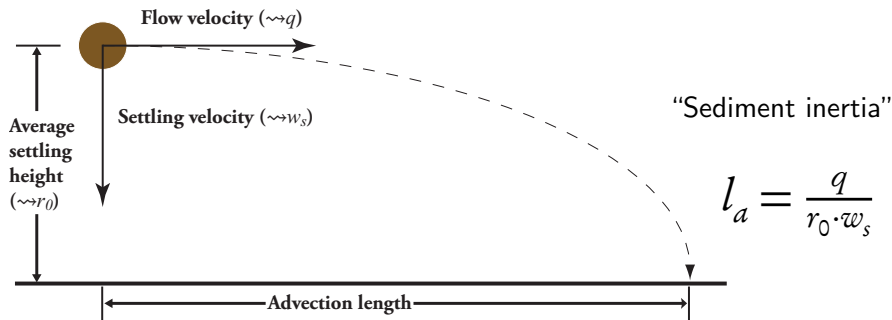
$$\frac{dq_s}{dx} = w_s \cdot (e - c_b) = w_s \cdot \left( \frac{r_0 \cdot q_{sc}}{q} - \frac{c_b}{c} \cdot \frac{c \cdot q}{q} \right) = w_s \cdot \left( \frac{r_0 \cdot q_{sc}}{q} - \frac{r_0 \cdot q_s}{q} \right)$$

$$\left( \frac{q}{r_0 \cdot w_s} \right) \frac{dq_s}{dx} = q_{sc} - q_s \implies \text{Define: } l_a = \left( \frac{q}{r_0 \cdot w_s} \right) \implies \boxed{l_a \frac{dq_s}{dx} = q_{sc} - q_s}$$

$$\begin{cases} l_a \rightarrow 0 & : & q_s(x) = q_{sc}(x) \\ l_a \rightarrow +\infty & : & \frac{dq_s}{dx} = 0 \end{cases} \implies \begin{cases} (1 - \lambda_p) \cdot \frac{d\eta}{dt} = -\frac{dq_{sc}}{dx} \\ q_s(x) = q_{s_0} \end{cases}$$

### (3/3) Consequences

- $l_a \rightarrow 0$ : Deposition follows local transport capacity gradient, i.e. local flow dynamics and topography  $\Rightarrow$  requires more complete description of flow field;
- $l_a \rightarrow +\infty$ : Deposition follows inlet sediment flux.



From Lamb et al., 2010

# Outline

## 1 Why?

- Motivation
- Examples

## 2 How?

- Physical model
- Computational transcription

## 3 Results

- Advection length scales
- Influence of initial grain size distribution
- Computed lengths vs. literature

## 4 Conclusions

## (1/4) Assumptions

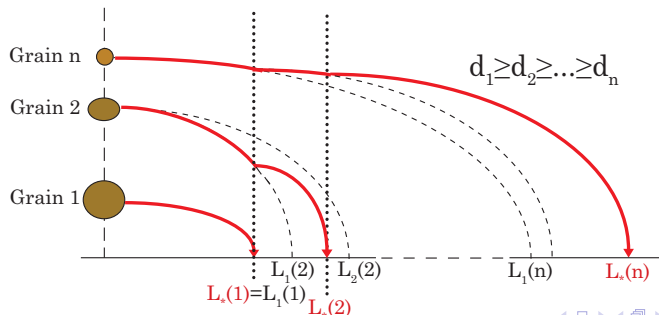
- Fully depositional flow  $\implies$  Primary reservoir objectives
- Simple advection length  $l_a$  computed for a single grain
- Concentration profile follows a Rouse profile at any time
  - Height of bedload layer  $Z_a \simeq 10 \cdot D_{50}$
  - Given center of mass of sediments (computed using  $Z_a$ , but with the Rouse number  $p$  for a single grain size)
  - Exponential decrease of concentration with distance
- Spherical grains, settling velocity from Dietrich, 1982 [4]
- Assumed value of drag coefficient  $C_f = 4 \times 10^{-3}$
- Fluid viscosities and densities either assumed or computed from temperature data



## (3/4) “Composite advection length”

When a distribution of grain sizes is involved, we assume:

- Constant flow velocity
- For one grain, same initial height  $Z_i$  independent of distribution:
  - Use advection length as settling velocity estimate, i.e.
  - Between deposition of grains  $i-1$  and  $i$ , grain  $n$  settles at velocity  $V_i(n) = \frac{Z_i(n) \cdot U_0}{L_i(d_n)}$ .



## (4/4) “Composite Advection Length”

The “Composite Advection Length” may be computed using recursive formulæ ( $d_1 > d_2 > \dots > d_n$ ):

$$\begin{cases} \frac{L_*(d_1)}{L_1(d_1)} = 1 \\ \frac{L_*(d_n)}{L_n(d_n)} = 1 + \sum_{j=1}^{n-1} L_*(d_j) \cdot \left[ \frac{1}{L_{j+1}(d_n)} - \frac{1}{L_j(d_n)} \right] \quad \forall n \geq 2 \end{cases}$$

Or, using a “ghost” grain size  $d_0$  of infinite mass:

$$\begin{cases} L_*(d_0) = 0 \\ L_*(d_n) = L_*(d_{n-1}) + L_n(d_n) \cdot \left[ 1 - \sum_{j=1}^{n-1} \frac{L_*(d_j) - L_*(d_{j-1})}{L_j(d_n)} \right] \quad \forall n > 0 \end{cases}$$

With:

- $L_*(d_i)$ : Composite advection length for grain  $d_i$
- $L_j(d_i)$ : Simple advection length for grain  $d_i$  between deposition of grain  $d_{j-1}$  and deposition of grain  $d_j$

# Outline

## 1 Why?

- Motivation
- Examples

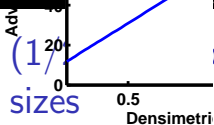
## 2 How?

- Physical model
- Computational transcription

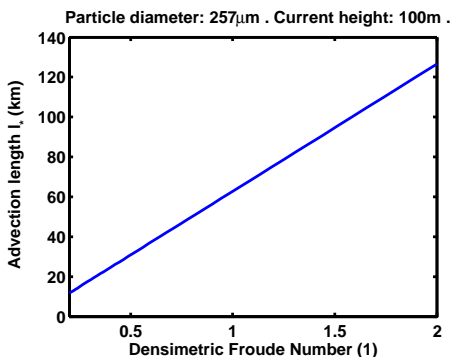
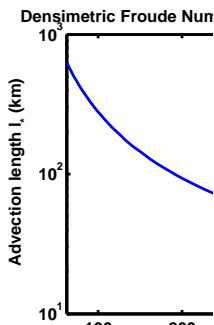
## 3 Results

- Advection length scales
- Influence of initial grain size distribution
- Computed lengths vs. literature

## 4 Conclusions



ous scales of advection length for small grain



## (2/2) Comparison with length scales of topographic elements

Location	Topographic element		size	Reference		
Monterey	Channel	Length	$300 + km$	Clark and Pickering, 1996b [5]		
Monterey	Channel	Width (min)	$0.4km$			
		Depth (min)	$32m$			
Monterey	Channel	Width (max)	$2.8km$			
Monterey	Channel	Depth (max)	$884m$			
Cascadia	Channel	Length	$2000 + km$	Clark and Pickering, 1996b [5]		
Cascadia	Channel	Width (max)	$5.6km$			
Cascadia	Channel	Depth (max)	$285m$			
Mississippi	Levees	Width Depth	$600m$ $10m$	Clark and Pickering, 1996a [6]		
NAMOC	Channel-levee system	Width	$10 < 30 < 40km$	Skene <i>et al.</i> , 2002 [7]		
		Depth	$100 < 200 < 300km$			
Laurentian					Width	$16 < 20 < 24km$
					Depth	$300 < 400 < 600m$
Amazon	Channel	Wavelength	$2 < 4.9 < 11km$	Pirmez and Imran, 2003 [8]		
		Radius of curvature	$0 < 1.05 < 3.5km$			

Table: Scales of some natural topographic elements

# Outline

## 1 Why?

- Motivation
- Examples

## 2 How?

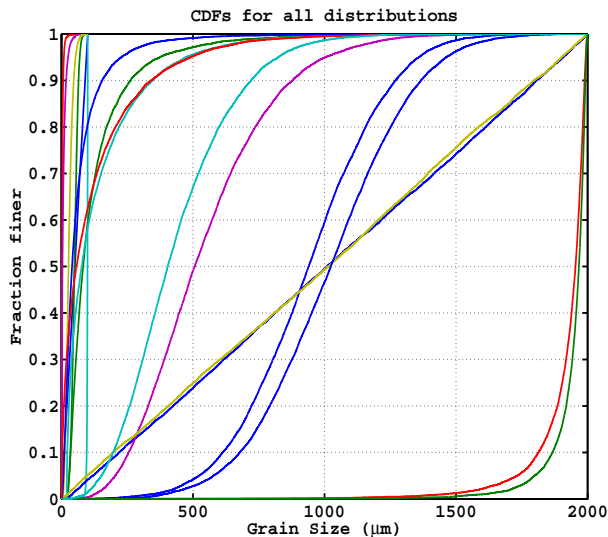
- Physical model
- Computational transcription

## 3 Results

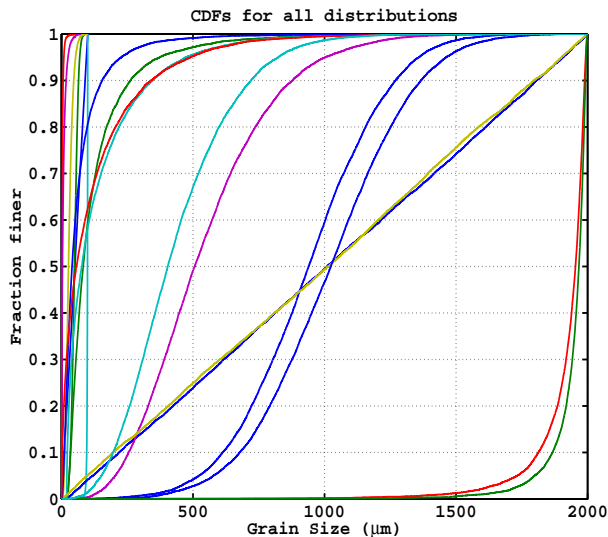
- Advection length scales
- Influence of initial grain size distribution
- Computed lengths vs. literature

## 4 Conclusions

# (1/3) Grain size distributions used to compute composite advection lengths



# (1/3) Grain size distributions used to compute composite advection lengths



18 distributions.

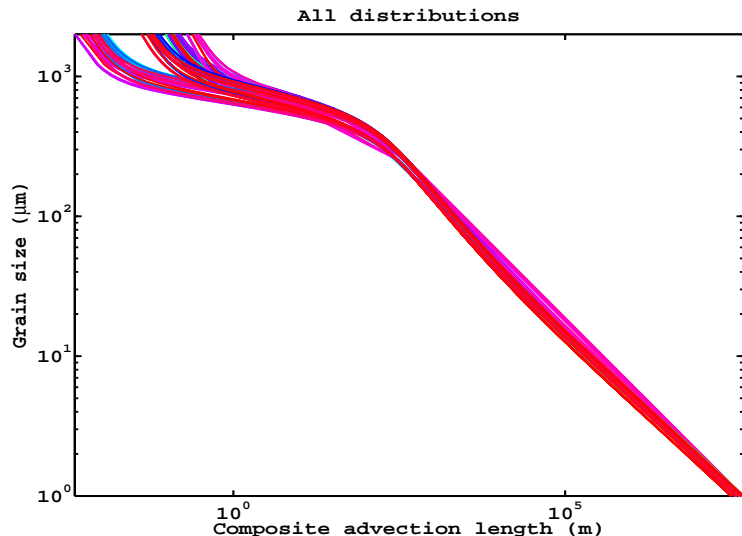
Shapes:

- 3× linear (uniform)
- 3× normal
- 3× lognormal
- 3× “Lognormal-opposite”
- 3× Gamma (small coefficient)
- 3× Gamma (large coefficient)

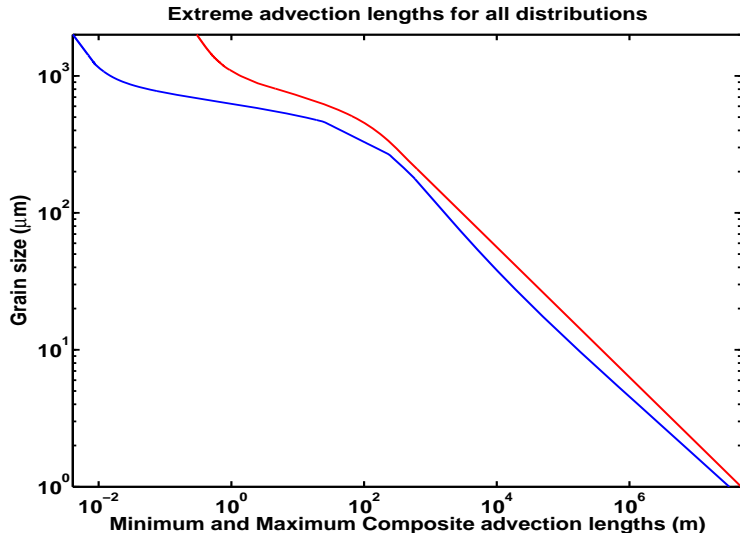
Ranges:

- 6 × [1; 100]  $\mu\text{m}$
- 6 × [20; 2000]  $\mu\text{m}$
- 6 × [1; 2000]  $\mu\text{m}$

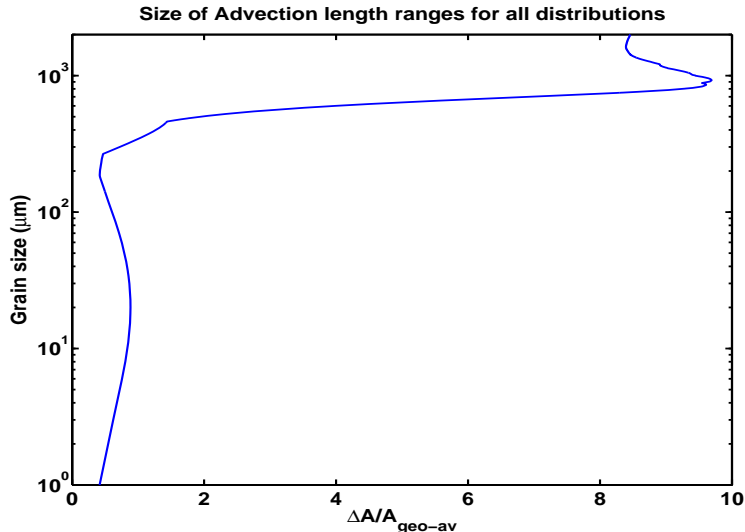
## (2/3) Collapse of small grain sizes on similar power-laws



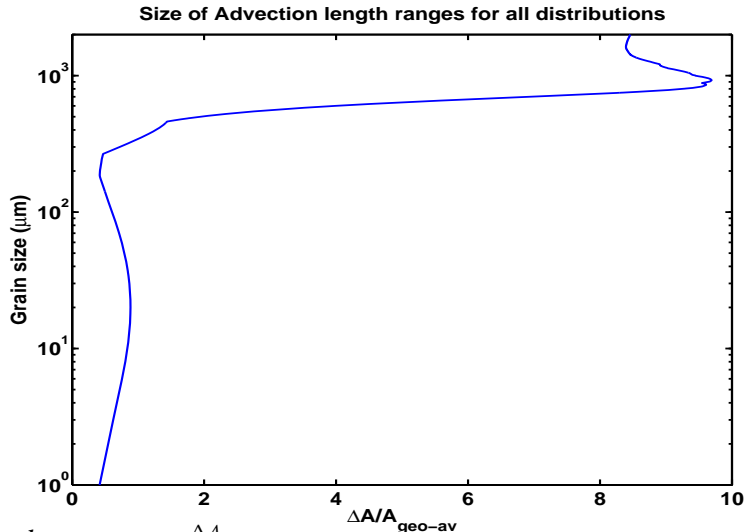
## (2/3) Collapse of small grain sizes on similar power-laws



## (2/3) Collapse of small grain sizes on similar power-laws



## (2/3) Collapse of small grain sizes on similar power-laws



For  $d \leq 324 \mu\text{m}$ ,  $\frac{\Delta A}{A_{\text{geo-av}}} < 0.89$

## (3/3) Remarks

- For grain sizes smaller than  $200\mu m$ , the initial grain size distribution bears little influence on a grain's advection length (Factor 2 is maximum).
- Mathematical viewpoint: System with stochastic input but deterministic process; "The smaller the grain size, the lesser the importance of the initial distribution of grain sizes."

# Outline

## 1 Why?

- Motivation
- Examples

## 2 How?

- Physical model
- Computational transcription

## 3 Results

- Advection length scales
- Influence of initial grain size distribution
- Computed lengths vs. literature

## 4 Conclusions

# García's 1994 experiments: Grain size distribution match

From García, 1994 [2]

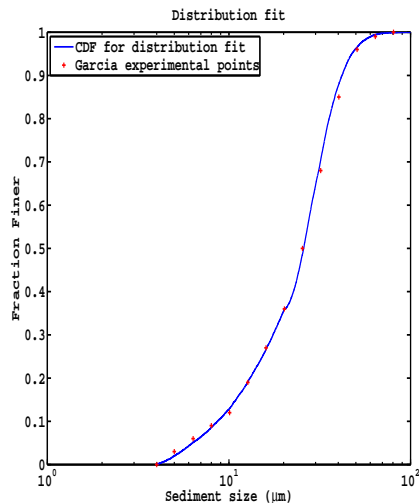
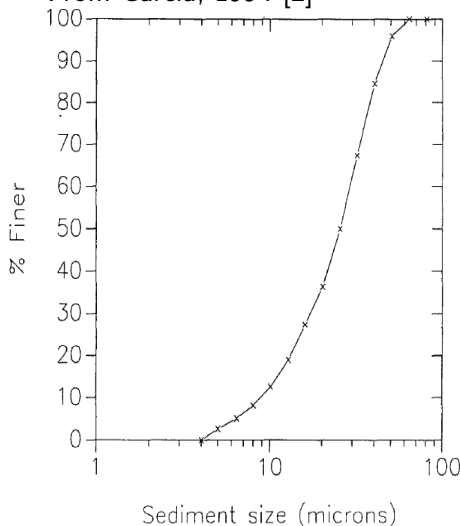


FIG. 3. Typical Size Distribution of Sediment Used in Experiments

# García's 1994 experiments: Grain size deposit match?

From García, 1994 [2]

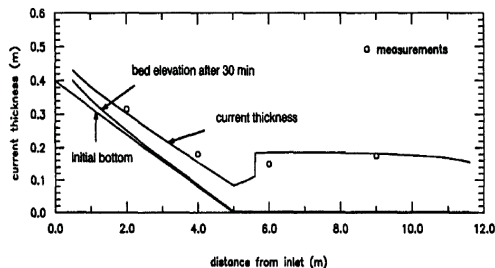


FIG. 15. Computed and Measured Current Thickness and Computed Bed Elevation for Run MIX6

# García's 1994 experiments: Grain size deposit match?

From García, 1994 [2]

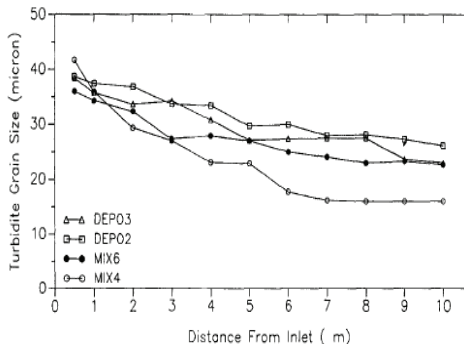
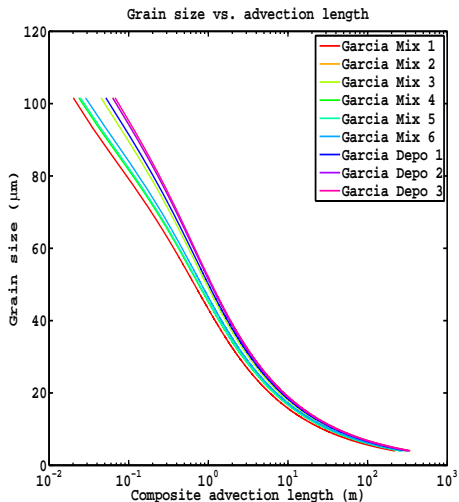


FIG. 8. Variation of Sediment Deposit Median Grain Size  $D_{50}$  with Distance from Inlet



# García's 1994 experiments: Grain size deposit match?

From García, 1994 [2]

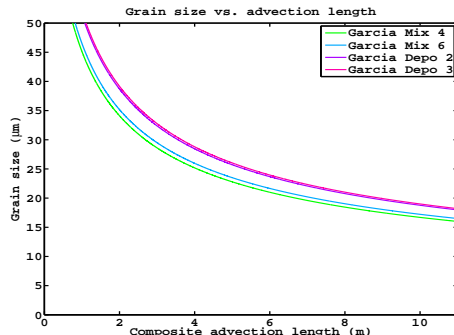
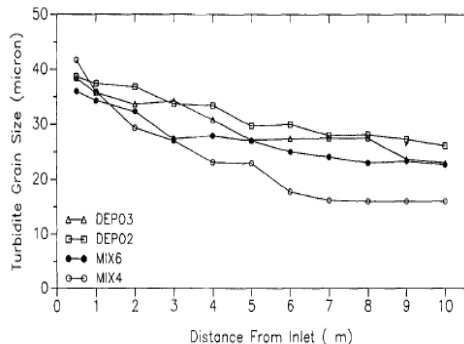
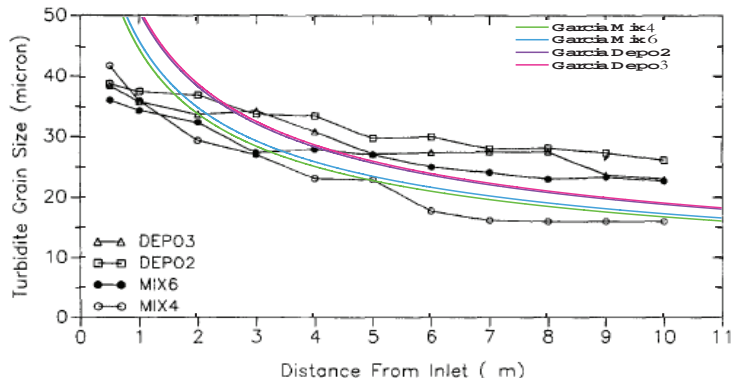


FIG. 8. Variation of Sediment Deposit Median Grain Size  $D_{50}$  with Distance f Inlet

# García's 1994 experiments: Grain size deposit match?

From García, 1994 [2]



**FIG. 8. Variation of Sediment Deposit Median Grain Size  $D_{50}$  with Distance from Inlet**

# Conclusions

- Advection-settling model simplifies modeling of turbidity current deposits
  - Complicated flow (with hydraulic jump, complex velocity profile) can create simple deposition profiles
  - Advection-settling already used to model levee growth by Straub and Mohrig, 2008 [9]
- Model is accurate for small grain sizes
- Comparison of advection length(s) and local scale(s) of topography indicates the need (or not) for more detailed modeling

# References I

- [1] Marcelo H. García.  
Hydraulic jumps in sediment-driven bottom currents.  
[Journal of Hydraulic Engineering-Asce](#), 119(10):1094–1117,  
1993.
- [2] Marcelo H. García.  
Depositional turbidity currents laden with poorly sorted sediment.  
[Journal of Hydraulic Engineering-Asce](#), 120(11):1240–1263,  
1994.
- [3] Michael P. Lamb, Brandon McElroy, Bryant Kopriva, John Shaw, and David Mohrig.  
Linking river-flood dynamics to hyperpycnal-plume deposits: Experiments, theory, and geological implications.  
[Geological Society of America Bulletin](#), in press.

# References II

- [4] William E. Dietrich.  
Settling velocity of natural particles.  
Water Resources Research, 18(6):1615–1626, 1982.
- [5] Julian D. Clark and Kevin T. Pickering.  
Submarine Channels: Processes and Architecture.  
Vallis Press, London, 1996.
- [6] Julian D. Clark and Kevin T. Pickering.  
Architectural elements and growth patterns of submarine channels: Application to hydrocarbon exploration.  
Aapg Bulletin-American Association of Petroleum Geologists, 80(2):194–221, 1996.

## References III

- [7] K. I. Skene, D. J. W. Piper, and P. S. Hill.  
Quantitative analysis of variations in depositional sequence thickness from submarine channel levees.  
Sedimentology, 49(6):1411–1430, 2002.
- [8] Carlos Pirmez and Jasim Imran.  
Reconstruction of turbidity currents in amazon channel.  
Marine and Petroleum Geology, 20(6-8):823–849, 2003.
- [9] Kyle M. Straub and D. Mohrig.  
Quantifying the morphology and growth of levees in aggrading submarine channels.  
Journal of Geophysical Research-Earth Surface, 113(F3), 2008.

# Questions?

## 5 Appendix

- Profile
- Data
- Plots
- Definitions

# Outline

## 5 Appendix

- Profile
- Data
- Plots
- Definitions

# Rouse profile: Presentation

Downward motion of sediment counteracted by upward eddy diffusion:

$$K_s(Z) \cdot \frac{dc_s}{dZ} = -w_s \cdot c_s \cdot (1 - c_s)$$

Separating variables and integrating between  $Z_a$  and  $Z$  gives:

$$\frac{dc_s}{c_s \cdot (1 - c_s)} = -p \cdot \frac{dZ}{Z} \Rightarrow \left[ \ln \left( \frac{c_s}{1 - c_s} \right) \right]_{Z_a}^Z = -p \cdot [\ln(Z)]_{Z_a}^Z$$

i.e.

$$\frac{c_s(Z)}{1 - c_s(Z)} = \frac{c_s(Z_a)}{1 - c_s(Z_a)} \cdot \left( \frac{Z}{Z_a} \right)^{-p}$$

with

- $K_s = \alpha \cdot \kappa \cdot u_* \cdot Z$
- $\kappa \simeq 0.407$ : Von Karman's constant,
- $u_* = \sqrt{C_f} \cdot \bar{u}$ : shear velocity,
- $\bar{u}$ : depth-averaged velocity,
- $C_f$ : Drag coefficient
- $p = \frac{w_s}{\alpha \cdot \kappa \cdot u_*}$ : Rouse number,
- $c_s(Z)$ : Average volume concentration in the flow at height  $Z$ ,
- $p < 0.8$ : Suspended load,
- Larger  $p$ : More and more bedload.

## Rouse profile: Center of mass of suspended sediment

If  $c_s \ll 1$ , then  $\frac{c_s}{1-c_s} \simeq 1$  and in the lower flow,  $c_s(Z) \simeq c_s(Z_a) \cdot \left(\frac{Z_a}{Z}\right)^p$ .  
Consequently,

$$Z_m = \frac{\int_{Z_a}^h c_s(Z) \cdot Z \, dZ}{\int_{Z_a}^h c_s(Z) \, dZ} \simeq \frac{1-p}{2-p} \cdot \frac{\left(\frac{Z_a}{h}\right)^p - \left(\frac{Z_a}{h}\right)^2}{\left(\frac{Z_a}{h}\right)^p - \frac{Z_a}{h}} \cdot h \quad p \notin \{1, 2\}$$

Therefore:

- if  $p \rightarrow +\infty$ , then  $Z_m = Z_a$ ;
- if  $p \rightarrow 0$ , then  $Z_m = \frac{h}{2}$ .

## Rouse profile: Characteristic distance above bed at which sediment diffuses in the flow

Using the approximation  $c_s(Z) \simeq c_s(Z_a) \cdot \left(\frac{Z_a}{Z}\right)^p$  in the lower flow,

$$\bar{c}_s \simeq \frac{1}{h} \cdot \int_{Z_a}^h c_s(Z) \, dZ = \frac{c_s(Z_a)}{1-p} \cdot \left[ \left(\frac{Z_a}{h}\right)^p - \frac{Z_a}{h} \right]$$

Hence the height associated with the average suspended sediment concentration:

$$c_s = \bar{c}_s \implies c_s(Z_a) \cdot \left(\frac{Z_a}{Z_*}\right)^p = \frac{c_s(Z_a)}{1-p} \cdot \left[ \left(\frac{Z_a}{h}\right)^p - \frac{Z_a}{h} \right]$$

i.e.

$$Z_* = \frac{Z_a}{\sqrt[p]{\frac{1}{1-p} \cdot \left[ \left(\frac{Z_a}{h}\right)^p - \frac{Z_a}{h} \right]}} \quad p \notin \{0, 1\}$$

## Rouse profile: Equation used by Rouse

The equation:

$$\frac{c_s(Z)}{1 - c_s(Z)} = \frac{c_s(Z_a)}{1 - c_s(Z_a)} \cdot \left( \frac{Z}{Z_a} \right)^{-p}$$

does not show that  $c_s(h) = 0$ . This equation may be replaced by the one given by Rouse:

$$c_s(Z) = c_s(Z_a) \cdot \left[ \left( \frac{h - Z}{Z} \right) \cdot \left( \frac{Z_a}{h - Z_a} \right) \right]^p$$

with  $p = \frac{w_s}{\chi \cdot u_*}$ , which is the equation used by Straub and Mohrig [9] to compute the advection length of sediments being transported over levees in decelerating, depositional currents.

# Outline

## 5 Appendix

- Profile
- Data
- Plots
- Definitions

# García input data

Run	$U_0$ ( $cm \cdot s^{-1}$ )	$h_0$ ( $cm$ )	$C_0$ (1)	$R_{i_0}$ (1)	$T_{inlet}$ ( $^{\circ}C$ )	$T_{flume}$ ( $^{\circ}C$ )	Run time ( $min$ )
MIX1	13.3	3	3.64	0.10	17.0	16.5	45
MIX2	13.3	3	7.28	0.20	4.0	15.0	43
MIX3	13.3	3	7.28	0.20	7.5	7.5	34
MIX4	11.0	3	6.42	0.26	6.5	7.0	20
MIX5	11.0	3	7.28	0.29	6.0	7.0	30
MIX6	11.0	3	10.90	0.44	4.5	5.0	30
DEPO1	13.3	3	3.64	0.10	6.0	7.0	40
DEPO2	14.3	3	21.80	0.52	6.8	7.5	24
DEPO3	14.3	3	10.90	0.26	6.0	6.0	24

**Table:** Input data for García's experiments ([2]).

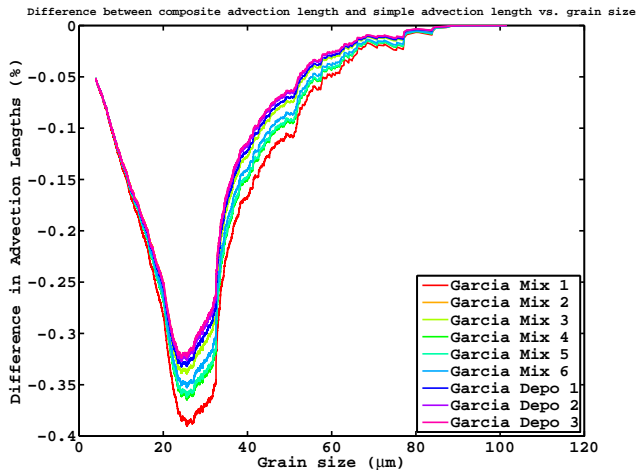
# Outline

## 5 Appendix

- Profile
- Data
- Plots
- Definitions

# García's 1994 experiments: Further simplifications?

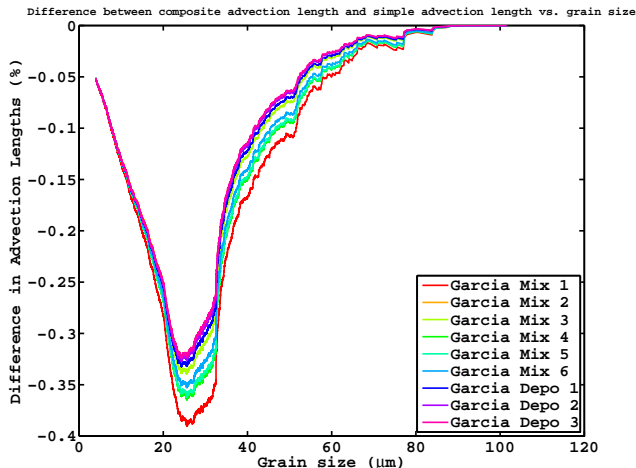
In these experiments, the grain sizes were small  
 $(\lesssim 100\mu m)$ :  $L_i(d_i) \simeq L_*(d_i)$ .



## García's 1994 experiments: Further simplifications?

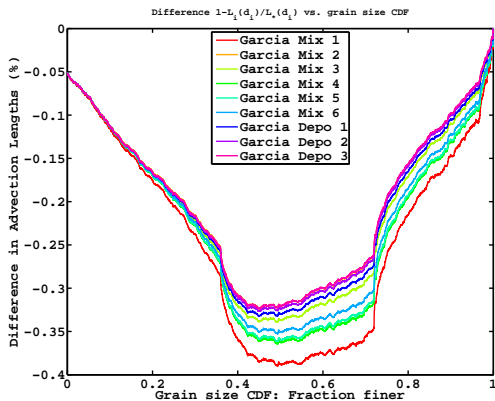
In these experiments, the grain sizes were small ( $\lesssim 100 \mu m$ ):  $L_i(d_i) \simeq L_*(d_i)$ .

However, the difference  $1 - \frac{L_i(d_i)}{L_*(d_i)}$  may reach more than 10% when the initial grain size distribution includes larger grains.



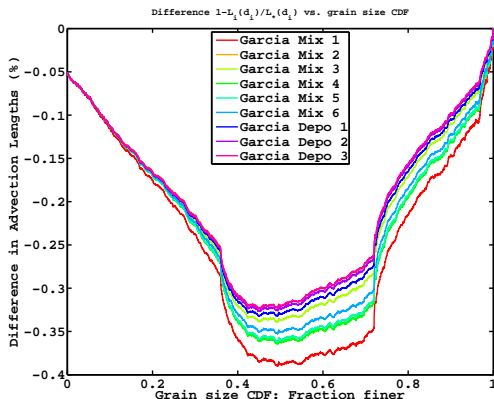
# Simple advection length as proxy for composite advection length

Replace the  $X$ -axis (grain size) with the  $Y$ -axis of the Cumulative Distribution function of grain sizes.



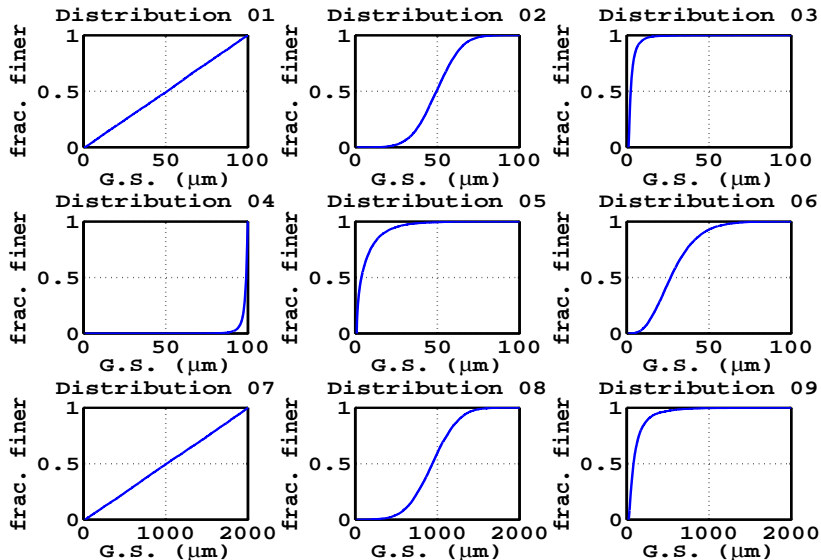
# Simple advection length as proxy for composite advection length

Replace the  $X$ -axis (grain size) with the  $Y$ -axis of the Cumulative Distribution function of grain sizes.

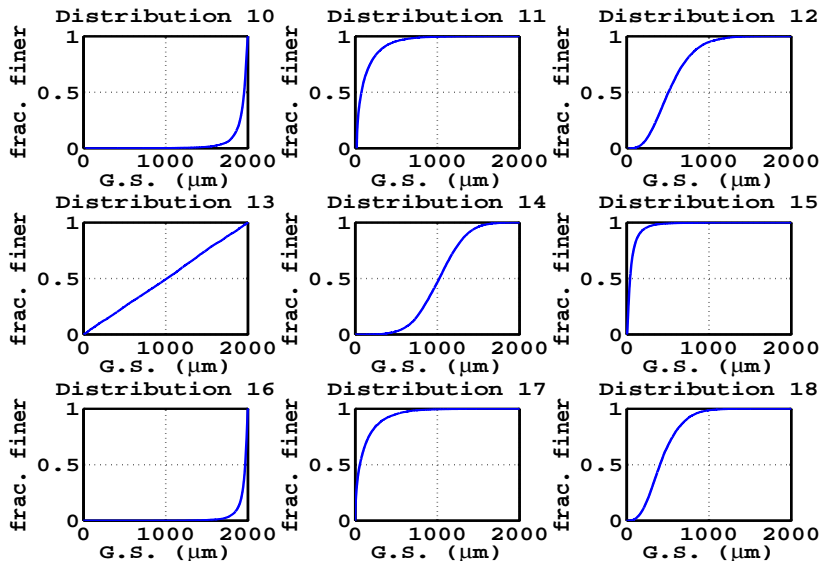


Similar behavior (drop in accuracy at mode) has been found using other distributions (normal, lognormal, gamma, etc.) with the same boundaries, with a noticeable exception for uniform distributions, where the drop in accuracy is skewed towards coarser grains.

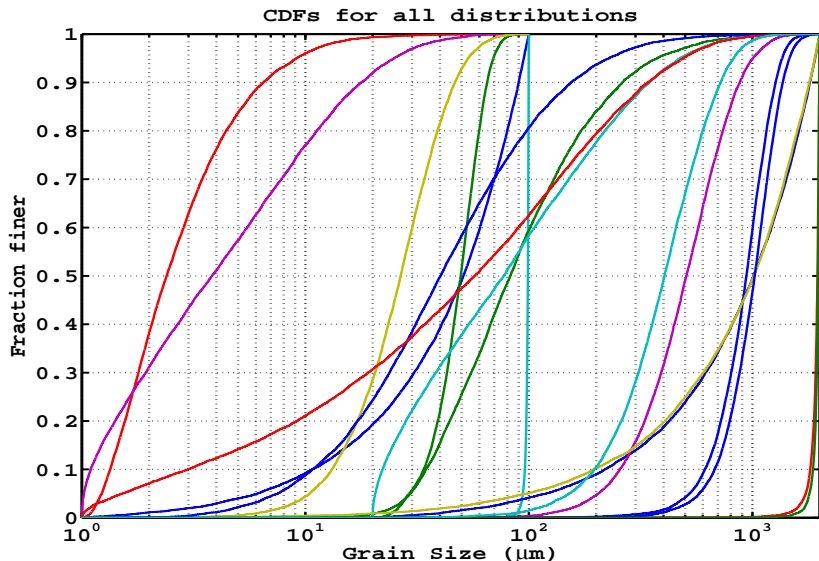
# (1/5) The 18 distributions: CDF plots



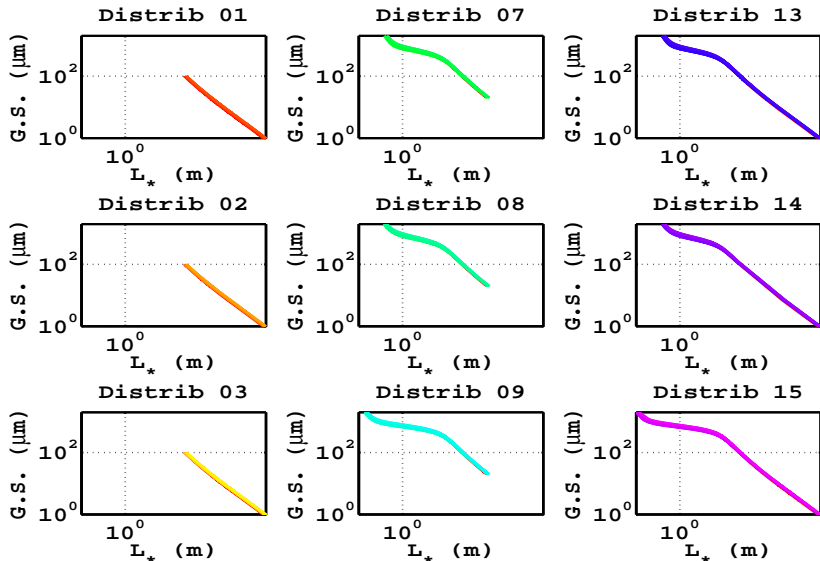
## (2/5) The 18 distributions: CDF plots



## (2/5) The 18 distributions: CDF plots, log scale...

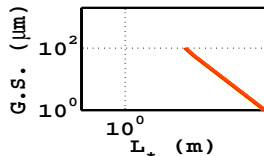


# (4/5) The 18 distributions: $T$ vs $d$

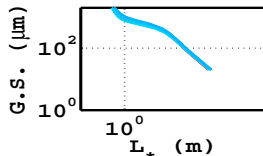


(5/5) The 18 distributions:  $T$  vs  $d$ 

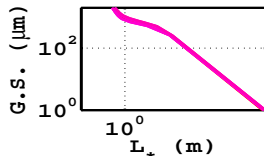
Distrib 04



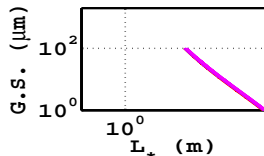
Distrib 10



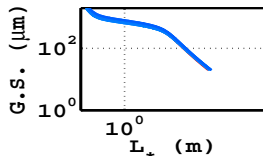
Distrib 16



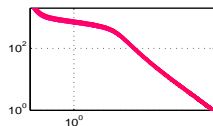
Distrib 05



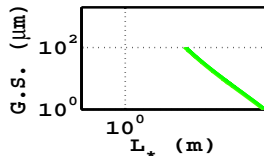
Distrib 11



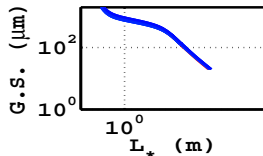
Distrib 17



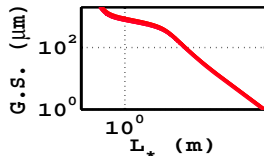
Distrib 06



Distrib 12



Distrib 18

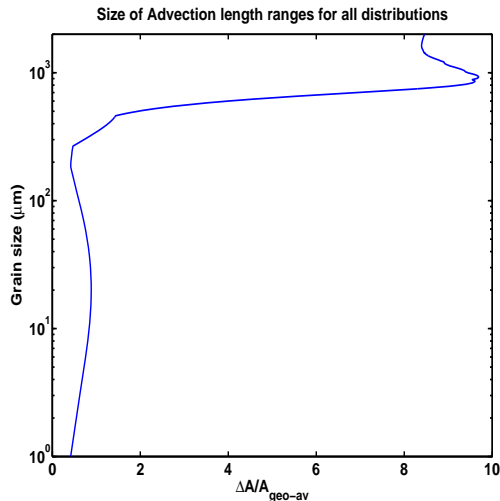


# Collapse of small grain sizes on similar power-laws

For  $d \leq 324 \mu m$ :

- $\frac{\Delta A}{A_{geo-av}} \leq 0.8840$
- $\frac{\Delta A}{A_{ar-av}} \leq 0.8085$
- $\frac{\Delta A}{A_{harm-av}} \leq 1.9330$
- $\frac{\Delta A}{\min(A)} \leq 1.3572$
- $\frac{\Delta A}{\max(A)} \leq 0.5758$

These values are reached for  $d = 20 \mu m$ .

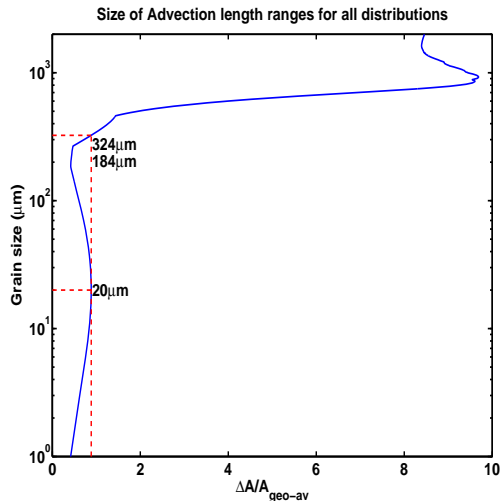


# Collapse of small grain sizes on similar power-laws

For  $d \leq 324 \mu m$ :

- $\frac{\Delta A}{A_{geo-av}} \leq 0.8840$
- $\frac{\Delta A}{A_{ar-av}} \leq 0.8085$
- $\frac{\Delta A}{A_{harm-av}} \leq 1.9330$
- $\frac{\Delta A}{\min(A)} \leq 1.3572$
- $\frac{\Delta A}{\max(A)} \leq 0.5758$

These values are reached for  $d = 20 \mu m$ .

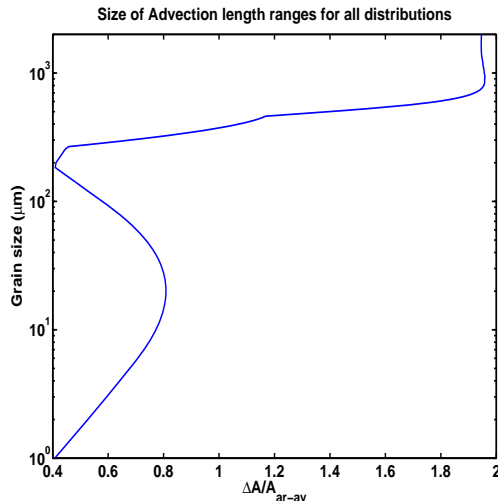


# Collapse of small grain sizes on similar power-laws

For  $d \leq 324 \mu m$ :

- $\frac{\Delta A}{A_{geo-av}} \leq 0.8840$
- $\frac{\Delta A}{A_{ar-av}} \leq 0.8085$
- $\frac{\Delta A}{A_{harm-av}} \leq 1.9330$
- $\frac{\Delta A}{\min(A)} \leq 1.3572$
- $\frac{\Delta A}{\max(A)} \leq 0.5758$

These values are reached for  $d = 20 \mu m$ .

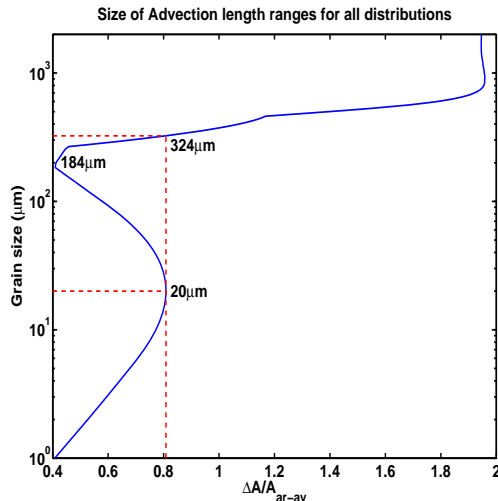


# Collapse of small grain sizes on similar power-laws

For  $d \leq 324 \mu m$ :

- $\frac{\Delta A}{A_{geo-av}} \leq 0.8840$
- $\frac{\Delta A}{A_{ar-av}} \leq 0.8085$
- $\frac{\Delta A}{A_{harm-av}} \leq 1.9330$
- $\frac{\Delta A}{\min(A)} \leq 1.3572$
- $\frac{\Delta A}{\max(A)} \leq 0.5758$

These values are reached for  $d = 20 \mu m$ .

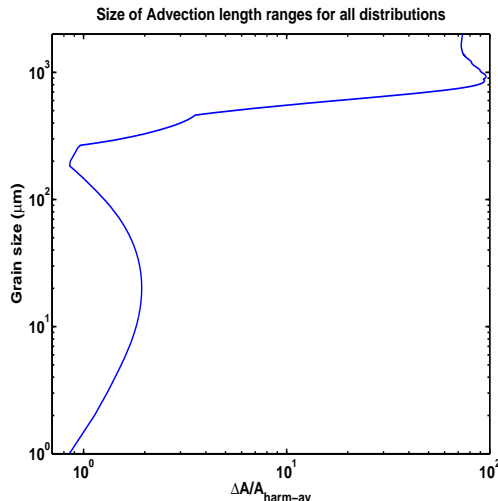


# Collapse of small grain sizes on similar power-laws

For  $d \leq 324 \mu m$ :

- $\frac{\Delta A}{A_{geo-av}} \leq 0.8840$
- $\frac{\Delta A}{A_{ar-av}} \leq 0.8085$
- $\frac{\Delta A}{A_{harm-av}} \leq 1.9330$
- $\frac{\Delta A}{\min(A)} \leq 1.3572$
- $\frac{\Delta A}{\max(A)} \leq 0.5758$

These values are reached for  $d = 20 \mu m$ .

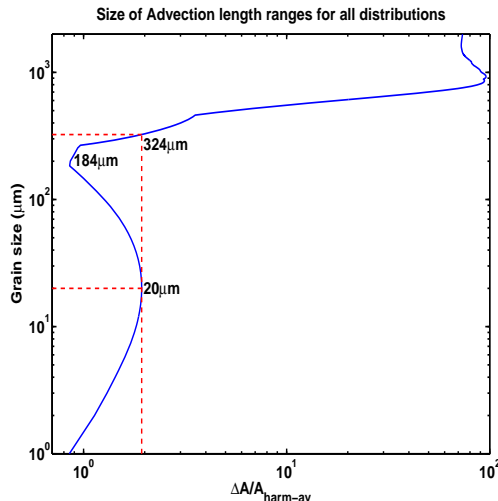


# Collapse of small grain sizes on similar power-laws

For  $d \leq 324 \mu m$ :

- $\frac{\Delta A}{A_{geo-av}} \leq 0.8840$
- $\frac{\Delta A}{A_{ar-av}} \leq 0.8085$
- $\frac{\Delta A}{A_{harm-av}} \leq 1.9330$
- $\frac{\Delta A}{\min(A)} \leq 1.3572$
- $\frac{\Delta A}{\max(A)} \leq 0.5758$

These values are reached for  $d = 20 \mu m$ .

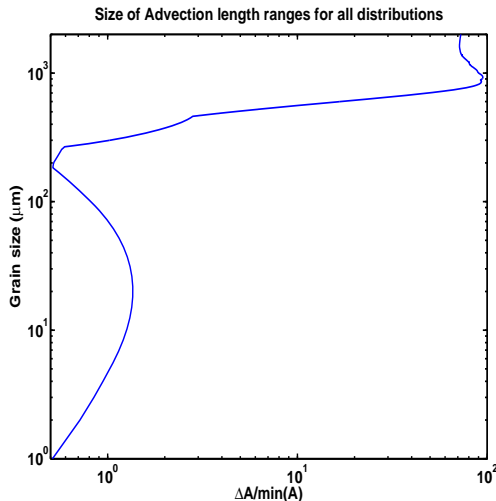


# Collapse of small grain sizes on similar power-laws

For  $d \leq 324 \mu m$ :

- $\frac{\Delta A}{A_{geo-av}} \leq 0.8840$
- $\frac{\Delta A}{A_{ar-av}} \leq 0.8085$
- $\frac{\Delta A}{A_{harm-av}} \leq 1.9330$
- $\frac{\Delta A}{\min(A)} \leq 1.3572$
- $\frac{\Delta A}{\max(A)} \leq 0.5758$

These values are reached for  $d = 20 \mu m$ .

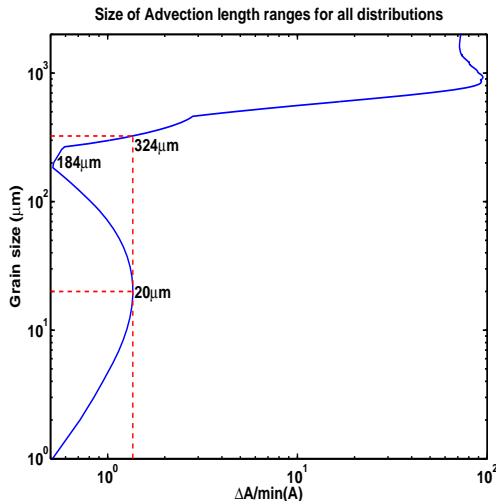


# Collapse of small grain sizes on similar power-laws

For  $d \leq 324 \mu m$ :

- $\frac{\Delta A}{A_{geo-av}} \leq 0.8840$
- $\frac{\Delta A}{A_{ar-av}} \leq 0.8085$
- $\frac{\Delta A}{A_{harm-av}} \leq 1.9330$
- $\frac{\Delta A}{\min(A)} \leq 1.3572$
- $\frac{\Delta A}{\max(A)} \leq 0.5758$

These values are reached for  $d = 20 \mu m$ .

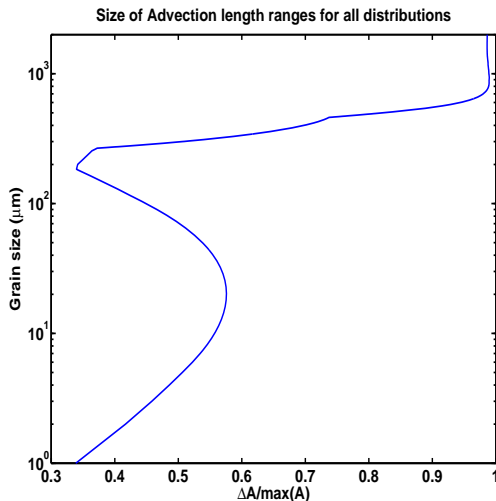


# Collapse of small grain sizes on similar power-laws

For  $d \leq 324 \mu\text{m}$ :

- $\frac{\Delta A}{A_{\text{geo-av}}} \leq 0.8840$
- $\frac{\Delta A}{A_{\text{ar-av}}} \leq 0.8085$
- $\frac{\Delta A}{A_{\text{harm-av}}} \leq 1.9330$
- $\frac{\Delta A}{\min(A)} \leq 1.3572$
- $\frac{\Delta A}{\max(A)} \leq 0.5758$

These values are reached for  $d = 20 \mu\text{m}$ .

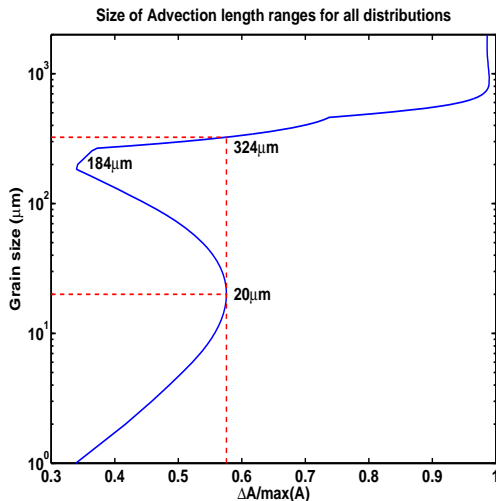


# Collapse of small grain sizes on similar power-laws

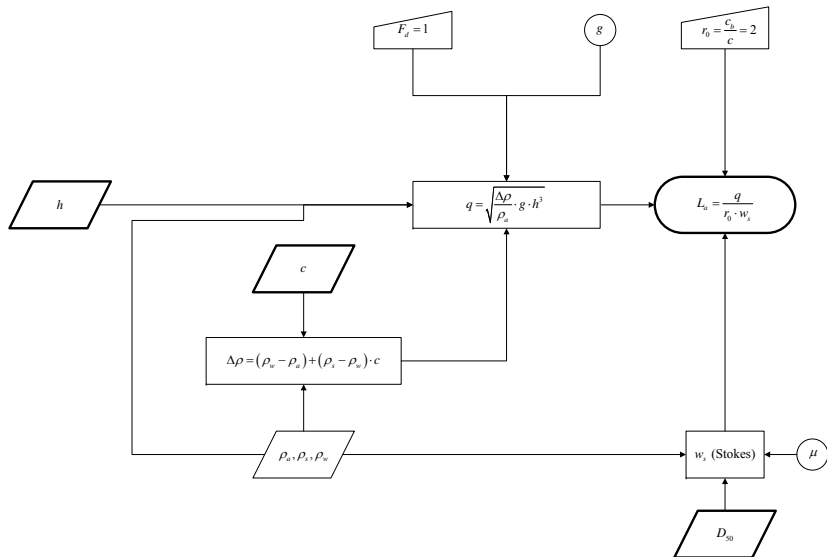
For  $d \leq 324 \mu m$ :

- $\frac{\Delta A}{A_{geo-av}} \leq 0.8840$
- $\frac{\Delta A}{A_{ar-av}} \leq 0.8085$
- $\frac{\Delta A}{A_{harm-av}} \leq 1.9330$
- $\frac{\Delta A}{\min(A)} \leq 1.3572$
- $\frac{\Delta A}{\max(A)} \leq 0.5758$

These values are reached for  $d = 20 \mu m$ .



# Alternate program “flowchart”



# Outline

## 5 Appendix

- Profile
- Data
- Plots
- Definitions

# Grain size scale

$mm$	$\phi$	Size class	
4096	-12	Boulder	Gravel
256	-8	Cobble	
64	-6	Pebble	
4	-2	Granule	
2	-1	Very coarse sand	
1	0	Coarse sand	Sand
0.5	1	Medium sand	
0.25	2	Fine sand	
0.125	3	Very fine sand	
0.0625	4		

**Table:** Grain size scale (Gravel and sand)

$\mu m$	$\phi$	Size class	
62.5	4	Coarse silt	Mud
31.25	5	Medium silt	
15.63	6	Fine silt	
7.813	7	Very fine silt	
3.9	8	Clay	
0.061	14		

**Table:** Grain size scale (Silt)

# Definitions

- Capacity: A flow is “at capacity” when the flux of sediment being transported by the flow at some location is equal to the sediment flux predicted by the local measure of boundary shear stress and particle size, fluid and sediment density, etc. at that location.

# Definitions

- Capacity: A flow is “at capacity” when the flux of sediment being transported by the flow at some location is equal to the sediment flux predicted by the local measure of boundary shear stress and particle size, fluid and sediment density, etc. at that location.
- “Law of the wall”: Relationship  $u(z) = \frac{u_*}{\kappa} \cdot \left( \frac{z}{z_0} \right)$  with
  - $u(z)$ : time-averaged velocity
  - $u_*$ : shear velocity
  - $z$ : height above bed
  - $z_0$ : roughness parameter,  $u(z_0) = 0$
  - $\kappa$ : von Karman’s constant,  $\kappa \simeq 0.407$